Self-assembly of carbon nanotubes into two-dimensional geometries using DNA origami templates

7 authors, including:

Hareem Maune

6 PUBLICATIONS 690 CITATIONS

SEE PROFILE

Si-Ping Han
California Institute of Technology

10 PUBLICATIONS 674 CITATIONS

SEE PROFILE

William A. Goddard
California Institute of Technology

1,664 PUBLICATIONS 130,213 CITATIONS

SEE PROFILE

Paul Wilhelm Karl Rothemund
California Institute of Technology

90 PUBLICATIONS 13,600 CITATIONS

SEE PROFILE

Some of the authors of this publication are also working on these related projects:

Structure and properties of energetic materials View project

Oxygen Reduction Reaction View project

Self-assembly of carbon nanotubes into two-dimensional geometries using DNA origami templates

Hareem T. Maune[†], Si-ping Han*[†], Robert D. Barish[†], Marc Bockrath, William A. Goddard III, Paul W. K. Rothemund and Erik Winfree

A central challenge in nanotechnology is the parallel fabrication of complex geometries for nanodevices. Here we report a general method for arranging single-walled carbon nanotubes in two dimensions using DNA origami—a technique in which a long single strand of DNA is folded into a predetermined shape. We synthesize rectangular origami templates (∼75 nm × 95 nm) that display two lines of single-stranded DNA 'hooks' in a cross pattern with ∼6 nm resolution. The perpendicular lines of hooks serve as sequence-specific binding sites for two types of nanotubes, each functionalized non-covalently with a distinct DNA linker molecule. The hook-binding domain of each linker is protected to ensure efficient hybridization. When origami templates and DNA-functionalized nanotubes are mixed, strand displacement-mediated deprotection and binding aligns the nanotubes into cross-junctions. Of several cross-junctions synthesized by this method, one demonstrated stable field-effect transistor-like behaviour. In such organizations of electronic components, DNA origami serves as a programmable nanobreadboard; thus, DNA origami may allow the rapid prototyping of complex nanotube-based structures.

Single-walled carbon nanotubes (SWNTs) have exceptional electronic properties that suggest their use in nanoscale information-processing devices. Towards this goal, there have been advances in SWNT synthesis[1], dispersion[2], sorting by electronic property[3] or length[4], and modification[5]. Methods for the parallel alignment of SWNTs have allowed the creation of lithographically defined high-performance electronic devices[6]. However, the arrangement of individual SWNTs into complex nanoscale geometries is an open challenge. Lithographic methods that produce the smallest arbitrarily complex patterns, such as dip-pen[7] and electron-beam[8], are serial processes; nanoimprint lithography can replicate such patterns[9], but methods for solving challenges such as alignment are still being developed[10]. Thus, although the organization of SWNTs by lithographically patterned affinity templates[11] or electrodes[12] could allow the creation of complex circuits, scaling up production remains difficult. Approaches based on protein and/or DNA self-assembly potentially provide parallelism. Many such methods have only created one-dimensional SWNT structures[13,14] and devices[15,16] in which a single SWNT positioned between a pair of electrodes is switched by the substrate back-gate. One method has created structures in which DNA linkers define the connectivity between three carbon nanotubes[17]; however, the angles between the nanotubes are uncontrolled. Two-dimensional control over SWNT organization is necessary to deterministically and reproducibly create circuits of many devices in which SWNTs gate other SWNTs directly.

DNA nanotechnology[18,19] provides, simultaneously, parallel and geometrically complex nanofabrication by making use of the binding specificity and structural predictability of nucleic acids. Over two decades ago, it was proposed[20] that DNA nanostructures could be used to template a three-dimensional memory. So far, DNA has been used to organize gold nanoparticles[21] into arrays and self-assemble one-dimensional SWNT electronic devices[15].

Scaffolded DNA origami[22] allows construction of arbitrary, ∼100 nm, two-dimensional shapes that can display desired patterns of 200 chemical modifications with ∼6 nm resolution. Trillions of origami can be self-assembled in millilitre reaction volumes in a single step. These properties suggest that DNA origami could be used to organize SWNTs into desirable device architectures[23–25]. Interfacing such circuits with the macroscale may require some top-down lithography, but the goal of using DNA templates is to shift more of the burden of creating complex geometries from lithography to self-assembly.

Cross-junction assembly scheme

Our approach is to align nucleic acid-labelled SWNTs (NL-SWNTs) along lines of complementary single-stranded DNAs (ssDNA) 'hooks'[26] on DNA origami. In principle, multiple populations of NL-SWNTs with different properties (for example, semiconducting or metallic) could be labelled with different sequences, and self-assemble simultaneously into a complex geometry defined by the layout of lines on an origami. Fortuitously, when ssDNAs are sonicated with SWNTs, they attach by means of physisorption of DNA bases to SWNT sidewalls[3] and cause the SWNTs to disperse[2] in aqueous solution. This non-specific interaction allows non-covalent attachment of DNA labels to SWNTs without disrupting their electronic properties[27] and provides a simple route to NL-SWNTs.

It is difficult, however, to design a DNA molecule that both disperses SWNTs and serves as an efficient label, because any ssDNA label it carries can also bind the SWNTs and either crosslink the SWNTs or become unavailable for binding hooks. Such SWNT-bound labels are capable of partial desorption and hybridization to free DNA hooks, but they do so prohibitively slowly[28]. In many applications such as those in which SWNTs are purposefully aggregated by DNA labels[29], it is only necessary that a fraction of DNA labels bind cognate hooks. However, to bind and align a SWNT

California Institute of Technology, Pasadena, California 91125, USA; [†]These authors contributed equally to this work. *e-mail: si-ping@wag.caltech.edu

with high fidelity to a row of relatively few DNA hooks on an origami it seems important that a high fraction of the SWNT labels bind. This suggests any DNA label intended to attach to the hooks must be protected from sticking to the SWNT, for example by making it double-stranded DNA (dsDNA). However, this presents the secondary challenge of removing the complementary 'protection strand' at the right time so that the DNA label can attach to hooks while remaining attached to the SWNT. Previous methods using protecting strands[30] or other secondary strands[31] do not protect ssDNA labels during critical assembly steps; thus these schemes appear to lack the level of control required for two-dimensional organization.

Here we prepare NL-SWNTs using a protection scheme borrowed from the construction of DNA nanomachines[32] and self-assemble them on DNA origami templates to create two-dimensional cross-junctions. In this scheme, protection strands are removed by the process of labels hybridizing to the origami hooks. Thus throughout our method, ssDNA labels remain almost completely protected until they bind the DNA origami; only short 'toehold' sequences are ever exposed as ssDNA. We created two types of NL-SWNTs (labelled 'blue' and 'red' for convenience) by using two different linkers to disperse separate aliquots of high-pressure CO conversion (HiPco) SWNTs (Fig. 1a). Each aliquot comprised a mixed population of semiconducting and metal SWNTs. In principle, pure populations of semiconducting and metallic SWNTs could be used to specify exclusive assembly of semiconductor–metal cross-junctions, the arrangement most likely to act as a field-effect transistor (FET.) Each linker is a two-stranded, partially duplex complex that adsorbs onto a SWNT via a 40-base poly-thymine (poly-T) dispersal domain. Its 20 nucleotide labelling domain (design methods in Supplementary Information, Text S1 and ref. 33) has a sequence specific to its colour and is complementary to similarly coloured hooks on a DNA origami template (Fig. 1b). A 15-base protection strand leaves 5 bases of the labelling domain unprotected. These 5 bases comprise the toehold, which is composed of locked nucleic acid (LNA). During dispersal, we expect the poly-T dispersal domain to adsorb on the SWNT while the protection strand prevents adsorption of the labelling domain. The relative instability of SWNTs dispersed by short ssDNA (4 or 6 nt)[34] suggests that the interaction of the short toeholds with the SWNT sidewalls is dynamic, making them available for binding hooks. (Short toeholds also seem important, because the use of 7 or 10-nt ssDNA toeholds resulted in crosslinked SWNTs during dispersal.) At the same time, the toehold is long enough that initiation of deprotection is still fast (toeholds should be ≥4 bases to maximize the reaction rate[35]). During assembly (Fig. 1c), a DNA hook complementary to all 20 labelling domain bases binds first to the 5-LNA-base toehold and initiates branch migration (Fig. 1d); this allows the hook to displace the protection strand and bind to the entire labelling domain[32,36]. We chose LNA for toeholds because branch migration efficiency increases with toehold binding stability[37], and LNA–DNA duplexes are more stable than their DNA counterparts.

Our template design (Fig. 1b, Supplementary Figs S1–S3 and Text S2) is based on the 'tall rectangle' origami[22], formed by ~200 DNA staples that fold a long scaffold strand into the desired sheet of B-form helices. The sequence of each staple (typically 32 bases) determines its unique position in the sheet. Hence, a DNA hook can be placed at any position by extending the 3′ end of the appropriate staple. DNA helical twist (10.5 bases per turn) determines the angle of the backbone relative to the plane of the origami; this allows hooks to be added to either face. We added a row of 11 red hooks to the bottom, and a column of 16 blue hooks to the top. In the original design, all staple ends fall on the bottom; thus, to project red hooks down, we concatenated the red hook sequence onto 3′ ends of staples in the desired row. For each staple in the blue column, we shifted the staple's 3′ end by half a turn (5 nucleotides) to position it on top and concatenated the blue hook sequence onto the end. Between each hook and staple sequence, we inserted a four-thymine spacer.

Origami aggregate by means of stacking interactions between helix ends along their vertical edges. Thus we omitted the leftmost column of staples from the original design[22]. This resulted in a column of single-stranded loops that inhibited stacking (Fig. 1b). Also, we replaced the rightmost column of staples with DNA strands that nucleated growth of a ~100-nm-wide, typically >500-nm-long, DNA ribbon (Fig. 1b) through algorithmic self-assembly of DNA tiles[38,39]. Addition of ribbons made image interpretation easier and appeared to increase the deposition rate of SWNT/DNA constructs.

Fidelity of alignment

To measure the efficiency, specificity and orientation of attachment for red and blue NL-SWNTs (independently) we imaged more than 200 SWNT/DNA constructs assembled using only red or blue SWNTs. Constructs were assembled by separately mixing either blue or red NL-SWNTs with templates displaying the cross-pattern of red and blue hooks (Fig. 1b). In each case, SWNTs had an opportunity to bind to either red or blue hooks. The desired outcome for each construct was a single SWNT aligned over the complementary hook array. Non-specific attachment would result in incorrect alignment or binding of more than one tube. Constructs were deposited on mica and scanned under buffer; 86% of templates mixed with red SWNTs had at least one SWNT attached, as did 80% of templates mixed with blue SWNTs. Of templates with attached SWNTs, ~25% were distorted or aggregated. Overall, ~50% of all templates were intact and had a single SWNT attached as desired. Figure 2 shows the distribution of alignments between templates and attached SWNTs. The angle of the ribbon with respect to the origami (Supplementary Information, Fig. S4a) allowed us to distinguish between red and blue faces and to define SWNT alignment angles. Figure 2 shows that the angular distribution for blue SWNTs peaks at ~0° (as expected) with 56% oriented within ±15° of the peak. The distribution of red SWNTs peaks at ~90° (as expected) with 50% within ±15° of the peak. These data suggest that NL-SWNTs strongly prefer their complementary hook array and align parallel to it. The importance of the protection strands for binding efficiency was verified in a control experiment: when blue SWNTs were prepared without protection strands <10% of DNA templates had SWNTs attached.

Cross-junctions

We assembled cross-junctions (Supplementary Text S3) by mixing templates with both red and blue NL-SWNTs simultaneously, and visualized them by atomic force microscopy (AFM) (Fig. 1e,f and Supplementary Fig. S5). Cross-junctions, like these examples, are frequently asymmetric because NL-SWNTs often bind near their ends (for unknown reasons), even appearing to align so that their ends are flush with the edge of the origami template. In the final constructs, red and blue NL-SWNTs are separated by a layer of DNA composed of their respective linkers (at least 1 nm where linkers attach due to the thickness of the poly-T dispersal domains, potentially up to a few nanometres depending on the detailed configuration of linkers) and the DNA origami (2 nm thick) that lies between them. AFM height measurements of the cross-junctions (~4 nm) provide a weak upper bound for the thickness of the layer given that we cannot measure the thickness of naked SWNTs for the exact structures in question. In principle, the intervening DNA layer is thicker, with the SWNT on opposite sides of the origami, and we chose this geometry over binding both SWNTs to the same side. We hypothesized that, if retained, a thicker intervening DNA layer might function as a better insulator
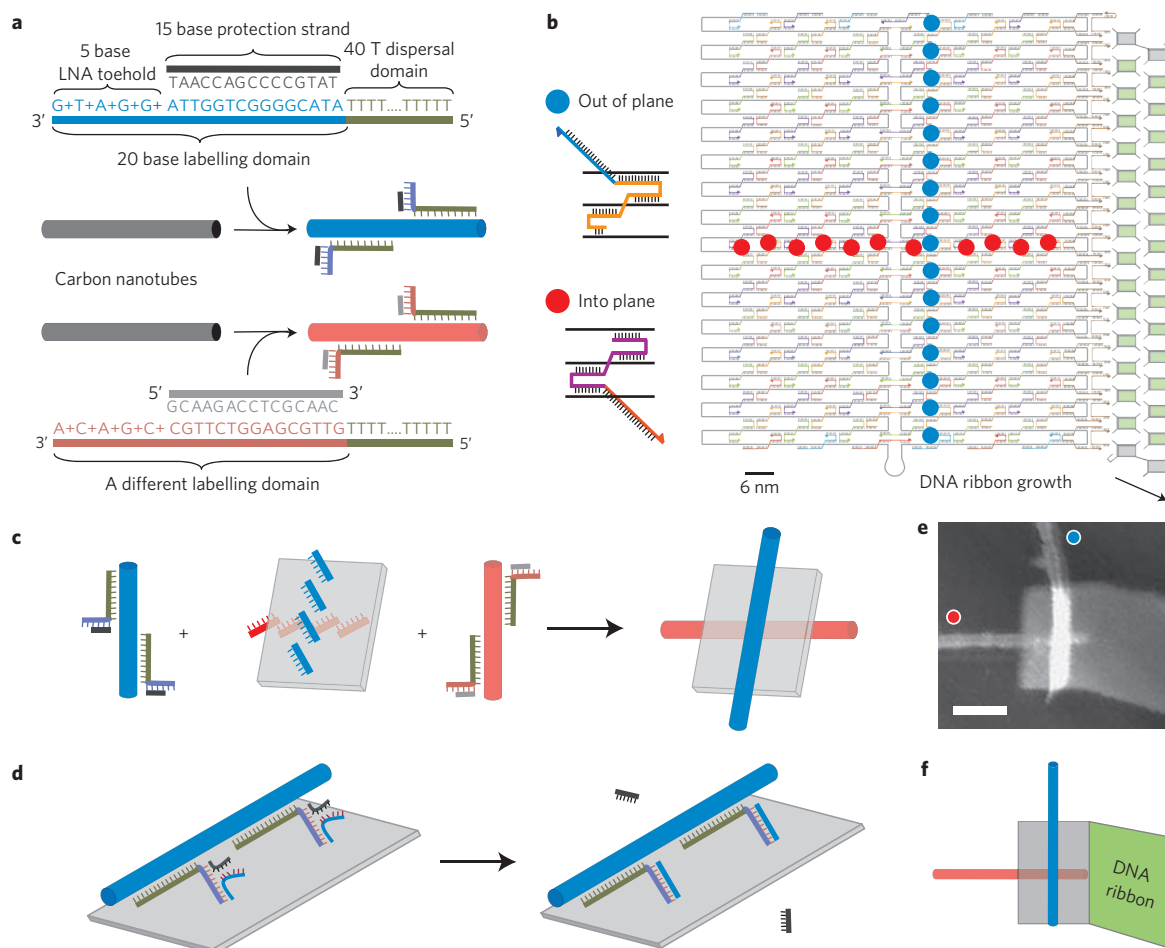
Figure 1 | Overview of cross-junction assembly. a, NL-SWNTs differ by linkers for which the labelling domains have different sequences. To distinguish them, SWNTs labelled with one sequence have been coloured red and those labelled with the other, blue. Dispersal domains bind linkers to SWNTs; labelling domains project into solution. **b**, A ~7,000-base long scaffold strand (grey) and ssDNA staples (multicoloured) form a rectangular origami template. Adapter strands (brown) on the right edge of the origami serve as nucleation sites for growth of a DNA ribbon (green/grey tiles). Red and blue dots indicate a pattern of hooks projecting from the origami. The insets show how staples are modified to carry hooks complementary to NL-SWNT labelling domains of corresponding colour; the scaffold is black. Red hooks project into the plane; blue hooks project out. **c**, Red and blue NL-SWNTs are mixed with a DNA template. They self-assemble sequence specifically with programmed orientations, red NL-SWNTs horizontally and blue NL-SWNTs vertically. **d**, The toehold on a linker initiates binding to a hook, leading to branch migration and release of the protection strand. Ribbons are not shown in **c** and **d**. **e**, A typical AFM height image of a cross-junction on mica under buffer; red and blue dots indicate NL-SWNT type. Scale bar, 50 nm. **f**, Schematic interpretation of **e** highlighting the relationship of origami, ribbon and SWNTs.

so that in the randomly occurring cases where one SWNT of the cross-junction was metallic and the other SWNT semiconducting, the metallic SWNT would more likely exert FET-type gating on the semiconducting SWNT. To look for possible FET behaviour, we electrically characterized several cross-junctions.

Cross-junctions were deposited on O_2 plasma-treated silicon wafers. Electrode fabrication and device measurement (Supplementary Text S5) was unreliable because the closely spaced ends of cross-junctions often required electrode placement with sub-50 nm precision and HiPco SWNTs have high intrinsic resistance. SWNT ends were contacted by palladium/gold electrodes fabricated using electron-beam lithography without post-fabrication thermal annealing, in an attempt to preserve the DNA template at the junction. DNA on SWNTs was selectively degraded in contact regions (but not at photoresist-protected cross-junctions) using an HCl rinse and 'DNA-AWAY' (Molecular BioProducts) surface decontaminant. Electrode fabrication was attempted for 23 cross-junctions; of these, six exhibited electrical conductance across one or both SWNTs and were further characterized by re-imaging and electrical measurements. Because the 17 non-conducting trials were not re-imaged,

it is unknown whether contacts were successfully made to these junctions.

Three of the six fully characterized devices showed FET-like behaviour; two were short-lived (Supplementary Fig. S9 shows FET behaviour in a short-lived device) and one had electronic properties stable over tens of up–down voltage cycles (Fig. 3 and Supplementary Fig. S8). For the stable device, the blue SWNT was used as the conduction channel and the red SWNT as the presumptive gate. Two-terminal I–V measurement across the source S and drain D electrodes of the blue SWNT (with $V_G = 0$) gave ~2 MΩ resistance in the ohmic region (Supplementary Fig. S8a). I–V measurements across the gate electrodes (G and g) of the red SWNT (with channel electrodes S and D left floating) gave ~6 GΩ resistance (Supplementary Fig. S8b). However the inter-SWNT tunnelling current (I_{GD} with S and g, floating) showed only ~3 MΩ of resistance when $V_{GD} < -0.5$ V (Supplementary Fig. S8c), indicating that the portion of the red SWNT leading from electrode G to the cross-junction is more conductive than implied by the measurement of I–V between G and g, and suggesting that the red SWNT–electrode g contact is responsible
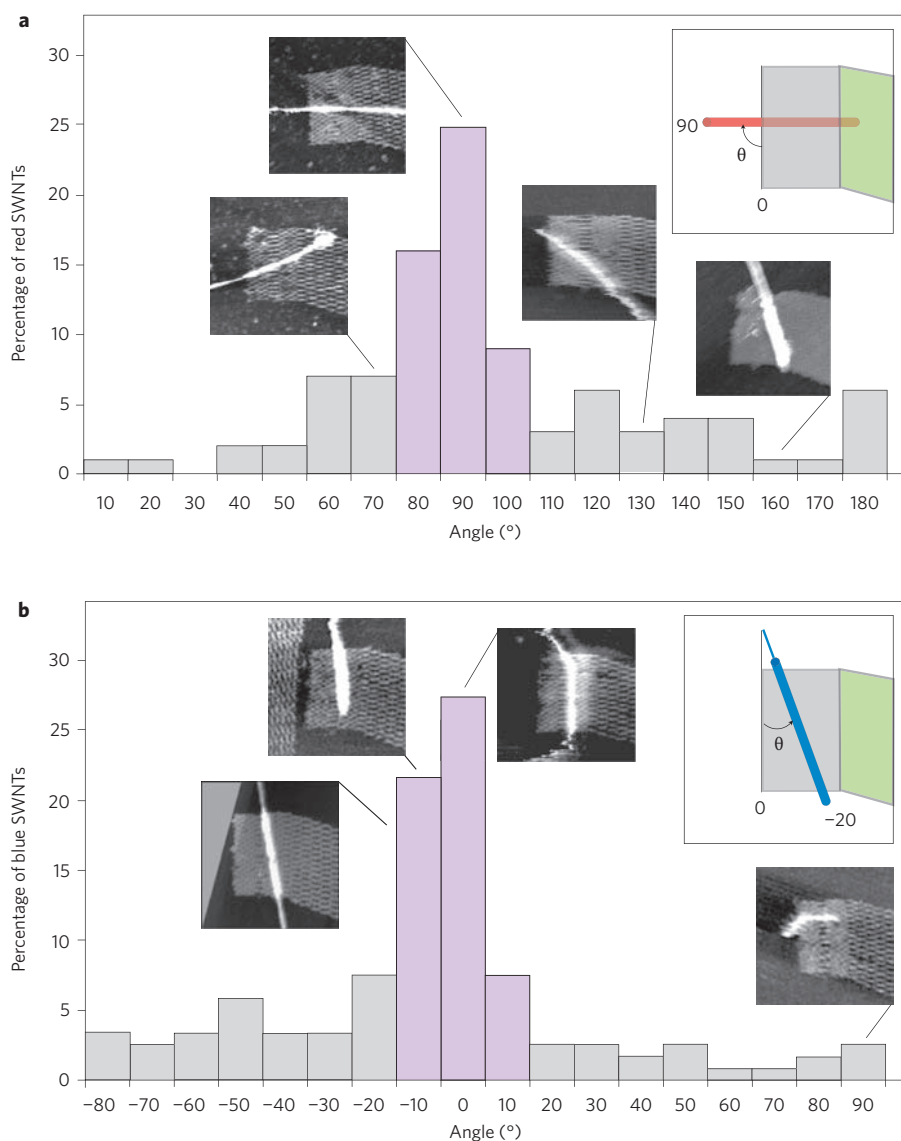
Figure 2 | Distributions showing sequence-specific attachment of NL-SWNTs to DNA templates and angular control over orientation. a,b, Randomly selected origami templates incubated with red or blue NL-SWNTs were imaged by AFM. Of these, 100 red NL-SWNT/template constructs (**a**) and 121 blue NL-SWNT/template constructs (**b**) were intact and had a single SWNT bound, ~50% of the total templates of each type. AFM images show examples of attachment at various angles. Insets in **a** and **b** show how SWNT angle was defined with respect to the origami's edge and ribbon orientation. Angles are defined similarly but the ranges are offset; angles of 100° to 180° in **a** corresponds to angles of −80° to 0° in **b**. For both distributions, ≥50% of tubes fall within ±15° (purple) of the desired angle. The third image from the left in **b** is flipped; unlike the others this structure landed blue face down.

for the high resistance between G and g. (It is extremely rare for all four contacts in such devices to be low resistance[40].)

For V_{GD} between +0.5 V and −0.5 V the resistance was high (the inter-SWNT tunnelling current was negligible, Supplementary Fig. S8c), providing a region in which the red SWNT could serve as a gate. Our intent had been that the DNA layer between the SWNTs would act as an insulator/dielectric to create this effect. However, for this device, we did not find an intact template after liftoff of the resist—we do not know whether any DNA (from the linker or origami) remained at the cross-junction. Thus, possible causes of the high-resistance region include remnant DNA, a Schottky barrier between the two SWNTs[41] or defects in the conduction path from G to D. In any case, an adequate conduction barrier was obtained. Finally, to test for FET behaviour, we swept the gate voltage V_{GD} (±0.5 V) at constant channel voltage ($V_{SD} = 0.85$ V) and observed that the channel current (I_{SD}) was

consistent with field-effect gating of a p-type semiconducting SWNT (Fig. 3d). The transconductance (dI_{SD}/dV_{Gg}) may contain contributions from the electric fields of both the red SWNT and electrode G (G was ~70 nm from the blue SWNT); quantification of these contributions and determination of the gating mechanism will require more sophisticated experiments such as scanned gate measurements[42].

Previous electrical characterization of crossed carbon nanotubes[40,41,43–46] includes the creation of CNT-gated CNT–FETs from crosses of semiconducting and metallic SWNTs with explicitly deposited SiO_2 dielectric layers[46] and the observation of rectification in cross-junctions formed by metal and semiconducting SWNTs[41]. Our stable device is not directly comparable to these devices because identification of the gate SWNT as a metal or semiconductor is ambiguous. However, the behaviour of the stable device falls within the range of behaviours previously reported.
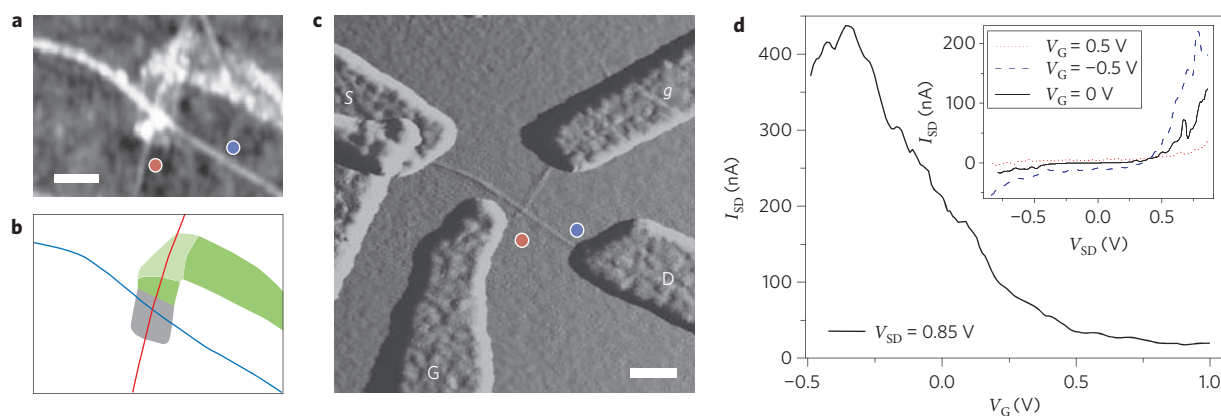
Figure 3 | Electrical characterization of a self-assembled SWNT cross-junction. a, AFM height image of an SWNT cross-junction on dry SiO_2 before electrode deposition. **b**, Interpretation of **a** indicating red and blue SWNTs, origami (grey), ribbon (dark green) and a place where the ribbon has folded back on itself (light green). Origami and ribbon contours are approximate; the origami-ribbon boundary, ribbon orienion, and colour of the top SWNT cannot be determined. **c**, AFM amplitude image of cross-junction from **a** with electron-beam patterned palladium/gold electrodes; the DNA template is no longer visible. Scale bars are 100 nm. Red and blue dots indicate NL-SWNT type, determined from ribbon orientation. Electrode labels: S, D, G and g. **d**, Source-drain current (I_{SD}) versus SWNT gate voltage (V_G) for a source-drain bias of 0.85 V. The current pre-amplifier used for measuring I_{SD} also served as a virtual ground. Inset shows the source-drain I–V for different gate biases.

Conclusions

We have demonstrated how DNA origami can be used to introduce two-dimensional geometry to the self-assembly of SWNT structures; our method should apply straightforwardly to other DNA nanostructures[19]. We have shown that SWNT/DNA constructs can be transferred from solution to dry SiO_2 with their geometry and electronic function intact; thus our process may be compatible with other standard microfabrication techniques. High-resolution lithographic techniques need multiple steps to incorporate multiple materials—here we have organized two populations of SWNTs in a single step. Our method should allow the simultaneous nanoscale positioning and alignment of multiple populations of SWNTs (each with different properties) based on the sequence of their DNA linkers. Similarly, our process should allow the simultaneous incorporation of other materials that can be labelled by DNA (such as gold nanocrystals[21]); this may lead to composite structures with novel electronic, optical or electrochemical properties.

Many open questions (Supplementary Text S6) and challenges remain—some that are unique to the specific cross-junction devices prototyped here, and others that more generally address the DNA-based self-assembly approach. With respect to creating two-dimensional SWNT FETs there are two difficulties. The first is the low yield of randomly occurring metal–semiconductor cross-junctions. Pre-sorting SWNTs by electronic property[3] before linker attachment should enrich for the desired junction type. The second is a requirement for reproducible electrical behaviour at the junction. Reproducibility might be improved either through consistent removal of the DNA interlayer, or consistent preservation. DNA-wrapping of SWNTs has previously been shown to enhance performance of one-dimensional SWNT FETs when the DNA was used to direct the assembly of a high-κ dielectric[27]. A similar approach to dielectric fabrication might be combined with our method.

Perhaps more fundamentally, there are several challenges that limit the self-assembly yield of a desired geometry, limit our ability to make better-defined geometries, or limit our ability to integrate a device into the larger geometry of a circuit architecture. The first is to control the translation of SWNTs along the lines of DNA hooks. Currently, the DNA hooks only specify the angle and intersection points of SWNTs. SWNT ends occur at random positions which makes contacting to them difficult. Such control might be achieved by using end-functionalized SWNTs[13] and/or

using length-sorted SWNTs[4] for which the lengths match those of the lines. The second challenge is to reduce device aggregation. Aggregation occurs because the solution-phase self-assembly of SWNTs and templates allows multiple DNA templates to bind individual long SWNTs; it may be avoided by attaching SWNTs to templates only after the templates have been deposited. Random deposition would serve this purpose, but brings up the third challenge, that of localizing the devices to specific positions so that they may be conveniently integrated and 'wired up'. Recent efforts have demonstrated the localization of individual DNA origami on lithographically patterned substrates[47]. With solution of these three challenges our method might be extended to the synthesis of multi-SWNT memory circuits[48] or logic gates[49].

Methods

A detailed description of the experimental procedure can be found in the Supplementary Information.

Synthesis and purification of NL-SWNTs. Ultrasonic dispersal (Branson 2510 sonicator, 100 W, 90 min) of SWNTs used ~600 µl of 32 µM nucleic acid linker solution (0.1 M NaCl) for every 0.1 mg of SWNTs. After dispersal, the concentration of excess free linkers (which could poison later samples) was reduced by electrodialysis, and monitored by spectrophotometry or gel electrophoresis. In one typical experiment the post-purification concentration of free linker was reduced to 120 nM while the concentration of desired SWNT-attached linkers was 420 nM, a ratio of <1:3 (Supplementary Text S1). Batch variation was considerable; for example, concentrations of SWNT-attached linkers varied from 100 nM to 1 µM.

Synthesis and purification of origami/ribbons. Origami/ribbons were assembled with a 5:1 excess of staples:scaffold strands in Mg^{2+} buffer (40 mM Tris-acetate, 1 mM EDTA, 12.5 mM magnesium acetate, pH 8.3, 0.22 µm filtered) and ligated to covalently link adjacent short strands in the origami and ribbon[50]. This reduced origami/ribbon template fragmentation during deposition. Ligation introduced ATP, ligase and extra buffer components. These extraneous reactants were reduced by spin filtration and the Mg^{2+} buffer was exchanged to Na^+ buffer (0.75 M NaCl, 0.01 M Na_2HPO_4, pH ~ 8, 0.22 µm filtered) to avoid Mg^{2+}-dependent precipitation of NL-SWNTs in the next step. We have observed that dispersal in Mg^{2+} buffers results in lower concentrations of SWNTs than dispersal in Na^+ buffers and that SWNTs dispersed in Mg^{2+} buffers appear to aggregate more quickly; this was previously observed by Ming Zheng, personal communication.

Assembly of NL-SWNT/DNA constructs. To create NL-SWNT/DNA constructs, we mixed NL-SWNTs with ~0.5 nM origami/ribbon templates. The concentration of NL-SWNTs was not known but in this final assembly buffer the concentration of NL-bound linkers was 10–100 nM. We tried a variety of buffers and incubation temperatures, achieving best results at 25 °C, 0.75 M NaCl, 0.01 M Na_2HPO_4 (~pH 8). The fraction of templates with attached SWNTs increased with incubation

time. However, incubation times over 30 minutes sometimes resulted in aggregates of many templates and SWNTs, perhaps due to attachment of long SWNTs to multiple templates.

Deposition on silicon wafers. Cross-junctions were deposited on O_2 plasma-treated silicon wafers (capped by 0.3–1.0 μm thick SiO_2) from Mg^{2+} and Ni^{2+} salt solutions. Although the DNA origami/ribbons appeared twisted and folded under dry-mode AFM, the cross-junction geometry of SWNTs was typically intact (Supplementary Figs S6, S7). Within a 400-μm² area, we typically found 5–10 self-assembled cross-junctions.

References

1. Hata, K. *et al.* Water-assisted highly efficient synthesis of impurity-free single-walled carbon nanotubes. *Science* **306,** 1362–1364 (2004).
2. Zheng, M. *et al.* DNA-assisted dispersion and separation of carbon nanotubes. *Nature Mater.* **2,** 338–342 (2003).
3. Zheng, M. *et al.* Structure-based carbon nanotube sorting by sequence-dependent DNA assembly. *Science* **302,** 1545–1548 (2003).
4. Huang, X., McLean, R. S. & Zheng, M. High-resolution length sorting and purification of DNA-wrapped carbon nanotubes by size-exclusion chromatography. *Anal. Chem.* **77,** 6225–6228 (2005).
5. Deng, W.-Q., Matsuda, Y. & Goddard, W. A. Bifunctional anchors connecting carbon nanotubes to metal electrodes for improved nanoelectronics. *J. Am. Chem. Soc.* **129,** 9834–9835 (2007).
6. Cao, Q. & Rogers, J. A. Ultrathin films of single-walled carbon nanotubes for electronics and sensors: a review of fundamental and applied aspects. *Adv. Mater.* **21,** 29–53 (2009).
7. Piner, R. D., Zhu, J., Xu, F., Hong, S. & Mirkin, C. A. 'Dip-pen' nanolithography. *Science* **283,** 661–663 (1999).
8. Vieu, C. *et al.* Electron beam lithography: resolution limits and applications. *Appl. Surf. Sci.* **164,** 111–117 (2000).
9. Chou, S. Y., Krauss, P. R. & Renstrom, P. J. Imprint lithography with 25-nanometer resolution. *Science* **272,** 85–87 (1996).
10. Wu, W. *et al.* Sub-10 nm nanoimprint lithography by wafer bowing. *J. Am. Chem. Soc.* **8,** 3865–3869 (2008).
11. Wang, Y., Maspoch, D., Zou, S. & Schatz, G. C. Controlling the shape, orientation, and linkage of carbon nanotube features with nano affinity templates. *Proc. Natl Acad. Sci. USA* **103,** 2026–2031 (2006).
12. Diehl, M. R., Yaliraki, S. N., Beckman, R. A., Barahona, M. & Heath, J. R. Self-assembled, deterministic carbon nanotube wiring networks. *Angew. Chem. Int. Ed.* **41,** 353–356 (2002).
13. Williams, K. A., Veenhuizen, P. T. M., de la Torre, B. G., Eritja, R. & Dekker, C. Nanotechnology: carbon nanotubes with DNA recognition. *Nature* **420,** 761 (2002).
14. Lyonnais, S. *et al.* A three-branched DNA template for carbon nanotube self-assembly into nanodevice configuration. *Chem. Commun.* 683–685 (2009).
15. Keren, K., Berman, R. S., Buchstab, E., Sivan, U. & Braun, E. DNA-templated carbon-nanotube field effect transistor. *Science* **302,** 1380–1382 (2003).
16. Hazani, M. *et al.* DNA-mediated self-assembly of carbon nanotube-based electronic devices. *Chem. Phys. Lett.* **391,** 389–392 (2004).
17. Bourgoin, J. P. *et al.* Directed assembly for carbon nanotube device fabrication. *Int. Electron Devices Meet. (IEDM '06)* 1–4 (2006).
18. Seeman, N. C. Nucleic-acid junctions and lattices. *J. Theor. Biol.* **99,** 237–247 (1982).
19. Seeman, N. C. An overview of structural DNA nanotechnology. *Mol. Biotechnol.* **37,** 246–257 (2007).
20. Robinson, B. H. & Seeman, N. C. The design of a biochip: a self-assembling molecular-scale memory device. *Protein Eng.* **1,** 295–300 (1987).
21. Pinto, Y. Y. *et al.* Sequence-encoded self-assembly of multiple-nanocomponent arrays by 2D DNA scaffolding. *Nano Lett.* **5,** 2399–2402 (2005).
22. Rothemund, P. W. K. Folding DNA to create nanoscale shapes and patterns. *Nature* **440,** 297–302 (2006).
23. DeHon, A. Array-based architecture for FET-based, nanoscale electronics. *IEEE Trans. Nanotechnol.* **2,** 23–32 (2003).
24. Dwyer, C. *et al.* Design tools for a DNA-guided self-assembling carbon nanotube technology. *Nanotechnology* **15,** 1240–1245 (2004).
25. Avouris, Ph., Chen, J., Freitag, M., Perebeinos, V. & Tsang, J. C. Carbon nanotube optoelectronics. *Phys. Status Solidi B.* **243,** 3197–3203 (2006).
26. Ke, Y., Lindsay, S., Chang, Y., Liu, Y. & Yan, H. Self-assembled water-soluble nucleic acid probe tiles for label-free RNA hybridization assays. *Science* **319,** 180–183 (2008).
27. Lu, Y. *et al.* DNA functionalization of carbon nanotubes for ultrathin atomic layer deposition of high κ dielectrics for nanotube transistors with 60 mv/decade switching. *J. Am. Chem. Soc.* **128,** 3518–3519 (2006).
28. Jeng, E. S., Barone, P. W., Nelson, J. D. & Strano, M. S. Hybridization kinetics and thermodynamics of DNA adsorbed to individually dispersed single-walled carbon nanotubes. *Small* **3,** 1602–1609 (2007).
29. Chen, Y., Liu, H., Ye, T., Kim, J. & Mao, C. DNA-directed assembly of single-wall carbon nanotubes. *J. Am. Chem. Soc.* **129,** 8696–8697 (2007).
30. Li, Y., Han, X. & Deng, Z. Grafting single-walled carbon nanotubes with highly hybridizable DNA sequences: Potential building blocks for DNA-programmed material assembly. *Angew. Chem. Int. Ed.* **46,** 7481–7484 (2007).
31. Hwang, E.-S. *et al.* The DNA hybridization assay using single-walled carbon nanotubes as ultrasensitive, long-term optical labels. *Nanotechnology* **17,** 3442–3445 (2006).
32. Yurke, B., Turberfield, A. J., Mills, A. P., Jr, Simmel, F. C. & Neumann, J. L. A DNA-fuelled molecular machine made of DNA. *Nature* **406,** 605–608 (2000).
33. Seeman, N. C. *De novo* design of sequences for nucleic acid structural engineering. *J. Biomol. Struct. Dyn.* **8,** 573–581 (1990).
34. Vogel, S. R., Kappes, M. M., Hennrich, F. & Richert, C. An unexpected new optimum in the structure space of DNA solubilizing single-walled carbon nanotubes. *Chem. Eur. J.* **13,** 1815–1820 (2007).
35. Yurke, B. & Mills, A. P. Jr. Using DNA to power nanostructures. *Genet. Progr. Evol. Mach.* **4,** 111–122 (2003).
36. Panyutin, I. G. & Hsieh, P. Kinetics of spontaneous DNA branch migration. *Proc. Natl Acad. Sci. USA* **91,** 2021–2025 (1994).
37. Christensen, U., Jacobsen, N., Rajwanshi, V. K., Wengel, J. & Koch, T. Stopped-flow kinetics of locked nucleic acid (LNA)–oligonucleotide duplex formation: studies of LNA–DNA and DNA–DNA interactions. *Biochem. J.* **354,** 481–484 (2001).
38. Schulman, R. & Winfree, E. Synthesis of crystals with a programmable kinetic barrier to nucleation. *Proc. Natl Acad. Sci. USA* **104,** 15236–15241 (2007).
39. Barish, R. D., Schulman, R., Rothemund, P. W. K. & Winfree, E. An information-bearing seed for nucleating algorithmic self-assembly. *Proc. Natl Acad. Sci. USA* **106,** 6054–6059 (2009).
40. Gao, B., Komnik, A., Egger, R., Glattli, D. C. & Bachtold, A. Evidence for Luttinger-liquid behavior in crossed metallic single-wall nanotubes. *Phys. Rev. Lett.* **92,** 216804 (2004).
41. Fuhrer, M. S. *et al.* Crossed nanotubes junctions. *Science* **288,** 494–497 (2000).
42. Bachtold, A. *et al.* Scanned probe microscopy of electronic transport in carbon nanotubes. *Phys. Rev. Lett.* **84,** 6082–6085 (2000).
43. Postma, H. W. Ch., de Jonge, M., Yao, Z. & Dekker, C. Electrical transport through carbon nanotube junctions created by mechanical manipulation. *Phys. Rev. B* **62,** R10653–R10656 (2000).
44. Ahlskog, M., Tarkiainen, R., Roschier, L. & Hakonen, P. Single-electron transistor made of two crossing multiwalled carbon nanotubes and its noise properties. *J. Appl. Phys.* **77,** 4037–4039 (2000).
45. Park, J. W., Kim, J. & Yoo, K.-H. Electrical transport through crossed carbon nanotube junctions. *J. Appl. Phys.* **93,** 4191–4193 (2003).
46. Lee, D. S., Svensson, J., Lee, S. W., Park, Y. W. & Campbell, E. E. B. Fabrication of crossed junctions of semiconducting and metallic carbon nanotubes: a CNT-gated CNT–FET. *J. Nanosci. Nanotechnol.* **6,** 1325–1330 (2006).
47. Kershner, R. J. *et al.* Placement and orientation of individual DNA shapes on lithographically patterned surfaces. *Nature Nanotech.* **4,** 557–561 (2009).
48. Rueckes, T. *et al.* Carbon nanotube-based non-volatile random access memory for molecular computing. *Science* **289,** 94–97 (2000).
49. Bachtold, A., Hadley, P., Nakanishi, T. & Dekker, C. Logic circuits with carbon nanotube transistors. *Science* **294,** 1317–1320 (2001).
50. O'Neill, P., Rothemund, P. W. K., Kumar, A. & Fygenson, D. K. Sturdier DNA nanotubes via ligation. *Nano Lett.* **6,** 1379–1383 (2006).

Author contributions
H.T.M., S.H. and R.D.B. conceived of the project, designed the structures, conducted the experiments and took the measurements with advice and consultation from all authors. All authors contributed to writing the paper. M.B., W.A.G., P.W.K.R. and E.W. provided financial support.

Additional information
Supplementary information accompanies this paper at www.nature.com/naturenanotechnology. The authors declare competing financial interests: details accompany the full-text HTML version of the paper at www.nature.com/naturenanotechnology. Reprints and permission information is available online at http://npg.nature.com/reprintsandpermissions/. Correspondence and requests for materials should be addressed to S.H.